Fractionated versus Standard Continuous Light Delivery in Interstitial Photodynamic Therapy of Dunning Prostate Carcinomas

Zhengwen Xiao,[1,3] Steve Halls,[4] Dwayne Dickey,[2] John Tulip,[2] and Ronald B. Moore[1,3]

Abstract

Purpose: The study aims to compare the standard/continuous light delivery with fractionated light delivery for interstitial photodynamic therapy (PDT) of prostate cancer.

Experimental Design: Dunning R3327 prostate tumor models were established in male syngeneic rats. When tumors reached ~3,000 mm^3, animals were randomized to various treatment groups. Three hours after QLT0074 injection, tumors were illuminated by 690-nm light delivered by a computer-controlled switch, which sequentially directed light to one of the seven optical fibers in cycles. For comparison, tumors were treated with continuous illumination. Tumors treated with light-only served as control. Dynamic contrast-enhanced magnetic resonance imaging was used to monitor tumor perfusion changes before and after PDT.

Results: Tumor response (animal survival) to PDT with fractionated light delivery was PDT dose dependent in both tumor models. Rats bearing anaplastic tumor treated by fractionated light (PDT dose: 1.5 mg/kg QLT0074, 900 J light) had a median survival of 51 days with 25% tumor cures compared with that of 26 days with no tumor cure by continuous illumination ($P = 0.015$) and 14 days by light-only ($P = 0.0001$). Rats bearing well-differentiated tumor treated by fractionated light had a median survival of 82 days compared with 65 days by continuous illumination ($P = 0.001$) and 37 days by light-only. PDT with fractionated light generated a perfusion reduction of 80% compared with 52% for continuous illumination in well-differentiated tumors.

Conclusions: Fractionated light delivery is more effective than continuous light delivery in PDT of prostate cancer (solid tumors). These results warrant further investigation in clinical trials.

Prostate cancer is the most common malignancy in American men (1). Prostate-specific antigen screening protocols have led to the diagnosis of more prostate cancer in earlier stages. It also results in the diagnosis of clinically insignificant cancers that are often indolent and not likely to adversely affect the quality or length of the patient's life (2). To date, choice of the best treatment option for men with prostate cancer represents a considerable challenge because of lack of precise markers to distinguish low-risk patients from high-risk ones (3, 4). Photodynamic therapy (PDT) is an alternative treatment modality for many cancers and seems promising for patients with localized prostate cancer. PDT as used in most protocols would not be expected to be mutagenic and can be repeated without accumulative toxicity (5, 6).

PDT relies on a dual selective process in which a photosensitizer (nontoxic dye) localizes in target tissue or a tumor before being activated by targeted light. A rapid photochemical reaction occurs, yielding reactive oxygen species (predominantly singlet oxygen, $^1O_2$) derived from tissue oxygen, which leads to depletion of tissue oxygen (7–9). The photochemical-induced alteration in the cell membranes (lipid peroxidation) is cytotoxic and vasculotoxic and results in cytokine release, causing blood vessel stasis and further hypoxia. This initial hypoxic phase is reversible in the early stage of PDT, depending on fluence rate and fractionation (7, 10). However, the cumulative effects of the photochemical reactions lead to vascular collapse and blood flow shutdown, which ultimately causes tumor necrosis (11, 12). PDT efficacy depends on tissue photosensitizer concentration, light dose, fluence rate, and tissue oxygenation. To increase target tissue photosensitizer concentration, intraarterial delivery of photosensitizers has been investigated (13). Other strategies of improving tumor response include lowering fluence rate, fractionating light illumination, and increasing tumor oxygen tension during PDT (7–9, 14, 15). All of these strategies seem to work well. One of the limitations of using low fluence rate and fractionation is the prolonged treatment time. Clinical application of PDT generally seeks to minimize treatment time. This problem may be partially addressed with multifiber interstitial PDT in larger solid tumors, such as prostate cancer. Because prostate cancer

Authors' Affiliations: Departments of [1]Oncology and [2]Electrical Engineering, University of Alberta; [3]Department of Surgery and [4]Oncological Imaging, Department of Radiology, Cross Cancer Institute, Edmonton, Alberta, Canada

Received 6/26/07; revised 9/6/07; accepted 9/17/07.

Grant support: National Cancer Institute of Canada, Terry Fox Frontiers grant 11439 (R.B. Moore), and Alberta Heritage Foundation for Medical Research (R.B. Moore).

The costs of publication of this article were defrayed in part by the payment of page charges. This article must therefore be hereby marked *advertisement* in accordance with 18 U.S.C. Section 1734 solely to indicate this fact.

Requests for reprints: Ronald B. Moore, Department of Surgery, University of Alberta, 2D2 Walter Mackenzie Health Sciences Center, 8440-112 Street, Edmonton, Alberta, Canada T6G 2B7. Phone: 1-780-407-6330; Fax: 1-780-407-6331; E-mail: rmoore@cha.ab.ca.

doi:10.1158/1078-0432.CCR-07-1561

is usually multifocal, multiple optic fibers (up to seven) are inserted into the prostate to deliver light for interstitial PDT to the whole prostate (6, 13). With this technique, fractionated illumination can be achieved by a computer-controlled switch. Furthermore, the fibers can also be used to detect tissue fluorescence feedback, which makes real-time monitoring of the PDT process possible. This novel switched light delivery system (Tulip J., et al., U.S. patent 60/646/656) was tested in the present study for therapeutic effectiveness in two prostate tumor models and compared with the standard/continuous light delivery (light on all fibers without pause).

Solid tumor oxygenation varies from area to area within a tumor and is difficult to accurately measure (16, 17). However, there is a general consensus that local O_2 consumption rate and blood perfusion are the most crucial direct factors affecting PDT efficacy (18). Dynamic contrast-enhanced magnetic resonance imaging (DCE-MRI) and blood oxygen level–dependent MRI were previously shown to be sensitive tools for assessing tumor perfusion and oxygen changes during and after PDT or antivascular drug therapies (19–21). Therefore, in this study, DCE-MRI was used to evaluate tumor vascular response (blood perfusion change) to interstitial PDT.

Materials and Methods

Animal tumor models. All animal procedures were done in accordance with the Guidelines of the Canadian Council on Animal Care and under the approval of the University Animal Welfare Committee. The Dunning R3327 rat prostate adenocarcinoma, which arose spontaneously in a male Copenhagen rat, has several tumor sublines (22). The slower-growing R3327-H subline is well-differentiated and closely mimics the human prostate cancer biology. The R3327-AT subline is an anaplastic and faster-growing tumor. Previous studies have shown the H tumor to be well perfused and the anaplastic tumor to be poorly perfused with a hypoxic/necrotic center (12). With the animals anesthetized with 2% isoflurane in oxygen, donor R3327 tumor chunks (3-mm blocks) were implanted s.c. into the left flank of male Fischer × Copenhagen rats weighing 200 to 300 g (Charles River Laboratories). Latency periods of 20 weeks for well-differentiated tumors and 2 weeks for anaplastic tumors were typically observed before they became palpable. Tumor growth was measured by procedures previously described (23–25). When tumors reached ≥2 cm in diameter (~3 cm^3), animals were randomized to various treatment groups.

Photosensitizer. Liposome-formulated QLT0074 (benzoporphyrin derivative 1,3-diene C,D-diethylene glycol ester A ring, a gift from QLT, Inc.) was reconstituted with sterile water to 2 mg/mL of drug before use. QLT0074 is a member of the same chemical class as the approved photosensitizer verteporfin (26). Previous drug distribution studies showed that the highest tumor photosensitizer level was observed ~3 h postinjection (27). This interval between drug administration and light illumination is generally suggested for PDT of solid tumors (28).

Light delivery techniques. The traditional continuous light delivery method used in this study was similar to that previously reported (12, 24, 25). Light at 690 nm, from an argon-driven Ti-Sapphire laser (Spectra Physics), was split into seven beams of equal intensity and focused into 600-μm quartz optical fibers with 1.5-cm cylindrical diffusing tips. Seven fibers were inserted into the tumor at 8 to 10 mm apart through a template which defined a hexagonal pattern of equilateral triangles. Light fluence rates were maintained at ~90 mW per fiber. A universal light power meter (Melles Griot 13 PDC 01) was used to measure the light that was collected in an integrating sphere (Melles Griot 13 PDC 03) from each fiber before and after treatment, as well as from separate fiber during treatment. For the novel fractionated light delivery method, light at 690 nm from one or two diode laser sources

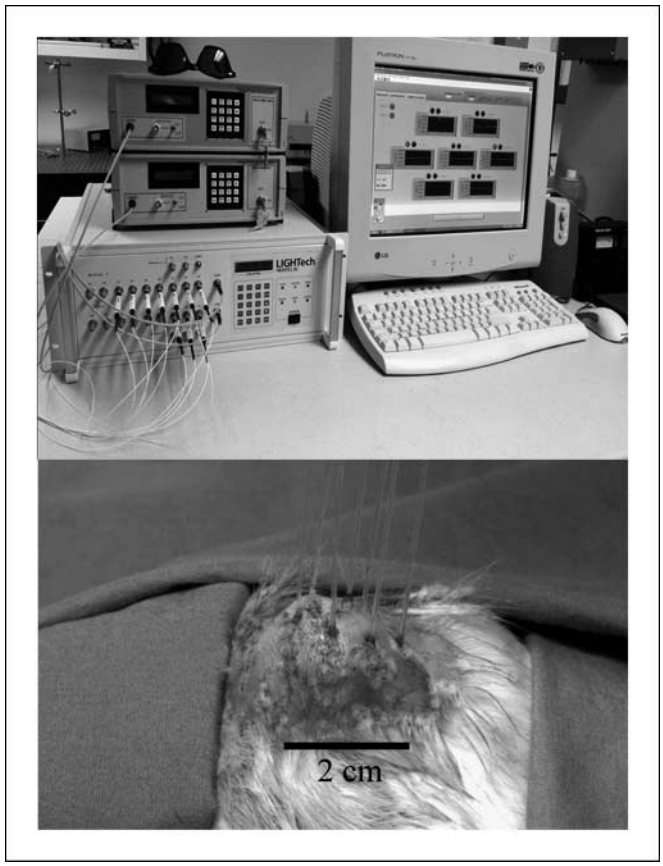

Fig. 1. Setup of the computer-controlled fractionated light delivery. *Top*, diode laser light is connected to the light switch that is controlled by a computer program (LabVIEW, National Instruments Corporate); *bottom*, the switch sequentially delivers light to the seven fibers implanted into the tumor. The length of light-on for each fiber is controlled by the computer.

(Optical Fiber Systems, Inc.) was delivered by a computer-controlled light switch with multiple output ports (Fig. 1). Light from the diode lasers was sequentially coupled to the fibers by the switch, with illuminating time of 1, 5, or 100 s for each fiber. The output fluence rate from each diode laser was ~200 mW per fiber. Identical to continuous light delivery, seven fibers were inserted through the template into the tumor. Thus, when one laser source was used and the light-on time was 100 s per fiber, then the light-off time for each fiber was 600 s. When two laser sources were used simultaneously, the light-off time was 300 s. Total light dose was 900 J per tumor for both continuous and fractionated light delivery. The time of treatment varied from ~25 min (continuous light delivery) to ~70 min (fractionated light delivery, one laser) or ~40 min (two lasers).

Interstitial photodynamic therapy. When tumors reached volumes of ~3 cm^3 (~2 cm in diameter), animals were randomly assigned to various treatment groups (see Table 1). Initially, dose-finding experiments were carried out with various fractionated light delivery protocols and graded doses of QLT0074. From these experiments, the maximum tolerated PDT dose of 2.0 mg/kg QLT0074 with 900 J light was determined. Therefore, the PDT dose for continuous light delivery was chosen as 1.5 mg/kg QLT0074 and 900 J. After the initial experiments, six groups of rats (9-15 per group; see Table 1) bearing anaplastic tumors were treated, including one group treated with light-only (900 J) as a sham control. Five groups of rats (8-12 per group) bearing well-differentiated tumors were treated and compared with the anaplastic tumors. QLT0074 was injected via the indwelling tail vein catheter 3 h before light illumination. During PDT, animals were anesthetized with ketamine (75 mg/kg, i.p.) and xylazine (8 mg/kg, i.p.) and kept

Table 1. Interstitial PDT of rat prostate tumors with fractionated or continuous light delivery

Treatment groups	No. rats	Tumor size, cm^3 mean ± (SD)	QLT-0074, mg/kg	Light* delivery method	No. death	No. cure	Median survival (d) †	*P* value versus continuous light delivery	HR (95% confidence interval)
Anaplastic tumor									
High dose	15	3.65 (1.5)	2.0	100-s on	5	2	66	0.0085	0.25 (0.29-0.70)
Medium A	12	2.17 (0.5)	1.5	100-s on	2	3	51	0.0157	0.29 (0.10-0.79)
Medium B	10	2.19 (0.5)	1.5	1-s on	1	1	35	0.2299	0.55 (0.21-1.4)
Low dose	10	2.98 (0.8)	1.0	100-s on	0	0	30	0.5974	1.28 (0.50-3.2)
Continuous	10	2.66 (0.6)	1.5	Nonstop	1	0	26	—	1
Light-only	9	3.12 (1.2)	0	1-100 s	1	0	14	0.0001	14.5 (3.9-53)
Well-differentiated tumor									
High dose ‡	12	3.43 (1.3)	2.0	100-s on	3	1	104	0.0009	0.17 (0.06-0.48)
Medium A	12	3.72 (1.2)	1.5	100-s on	2	2	82	0.001	0.28 (0.10-0.74)
Medium B	10	3.66 (0.9)	1.5	5-s on	1	0	95	0.0015	0.31 (0.12-0.80)
Continuous	10	3.44 (1.0)	1.5	Nonstop	0	0	65	—	1
Light-only	8	3.91 (1.5)	0	5-100 s	1	0	37	0.0029	6.82 (1.9-24)

*Light dose was 900 J per tumor; see Materials and Methods for details of light delivery.
† The median time for tumors to grow 4 times treatment volume post-PDT.
‡ Half of these rats were treated with two lasers simultaneously.

warm with a circulating warm-water blanket. The body was draped from light, except for the tumor. Four 27-gauge copper-constantan thermal couple needles (Omega) were inserted into the tumor along the tracks of the optic fibers to continuously monitor intratumor temperature during light illumination. After PDT, animals were subjected to MRI tumor perfusion studies.

DCE-MRI technique. The dynamic MRI perfusion studies of tumor were conducted before and 1 to 72 h post-PDT using a Philips Intera 1.5 T magnet MRI unit (Best). Two small C4 surface coils were used to detect the RF signals, with one underneath the anaesthetized rat and the other on the top (abdomen). At the same time of MRI scanning, gadoteridol (0.15 mmol/kg or 0.1 mL per rat) was slowly injected via the tail vein catheter, followed by a 0.9-mL normal saline flush (a total volume of 1 mL) over 30 s. Dynamic perfusion scanning used a coronal T1-weighed three-dimensional volume gradient echo technique [TR/TE = 7.5/4.4 ms, flip angle = 40, field of view = 160 × 160 mm, matrix of 196 × 256, 10 slices of slice thickness/gap = 3.5/0 mm, scan repetition time = 10 s for 10 repetitions (total scan time of 100 s, 100 images collected for each tumor)]. This was followed by post-gadoteridol T1-weighed spin echo imaging. The dynamic signal intensity of gadoteridol perfusion was calculated on a pixel-by-pixel basis from the whole tumor central section and from manually outlined regions of interest of the tumor periphery. Signal intensity curves were graphed as gadoteridol-induced enhancement versus time, using the averaged results from the rats of each treatment group. Comparisons between pretreatment and posttreatment measurements and between fractionated and continuous light delivery groups were done using two-tailed Student's *t* test or one-way ANOVA (SAS ver. 9.1, SAS Institute, Inc.).

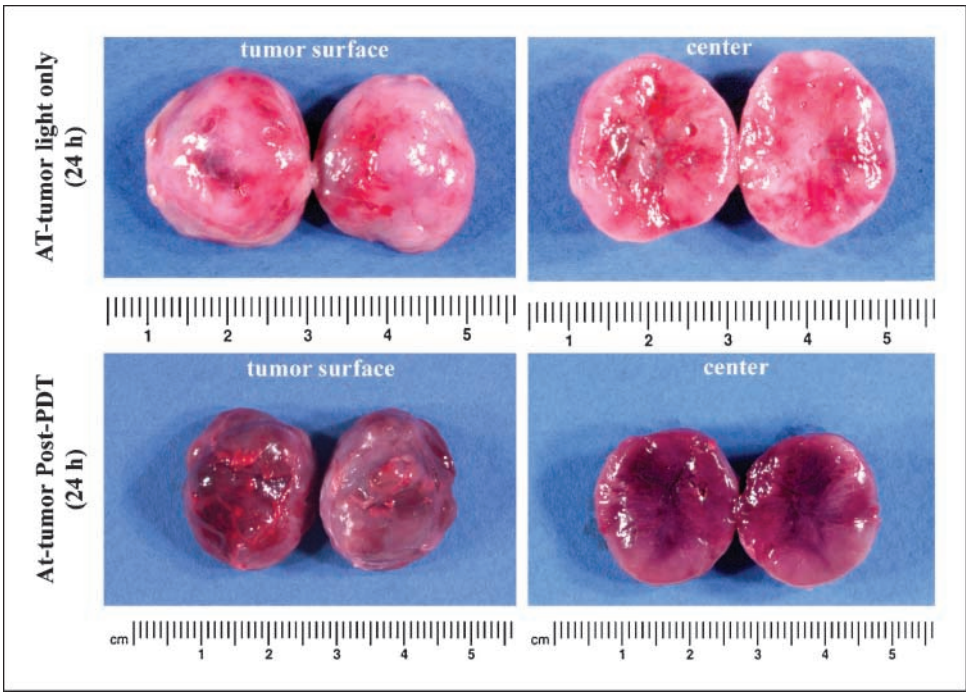

Fig. 2. Gross pictures of anaplastic (*AT*) tumors treated by 900 J light-only (*top*) or by interstitial PDT with fractionated light delivery and 2 mg/kg QLT0074 (*bottom*). Marked hemorrhagic change is observed in the whole tumor 24 h post-PDT but not in the tumor treated with light-only.

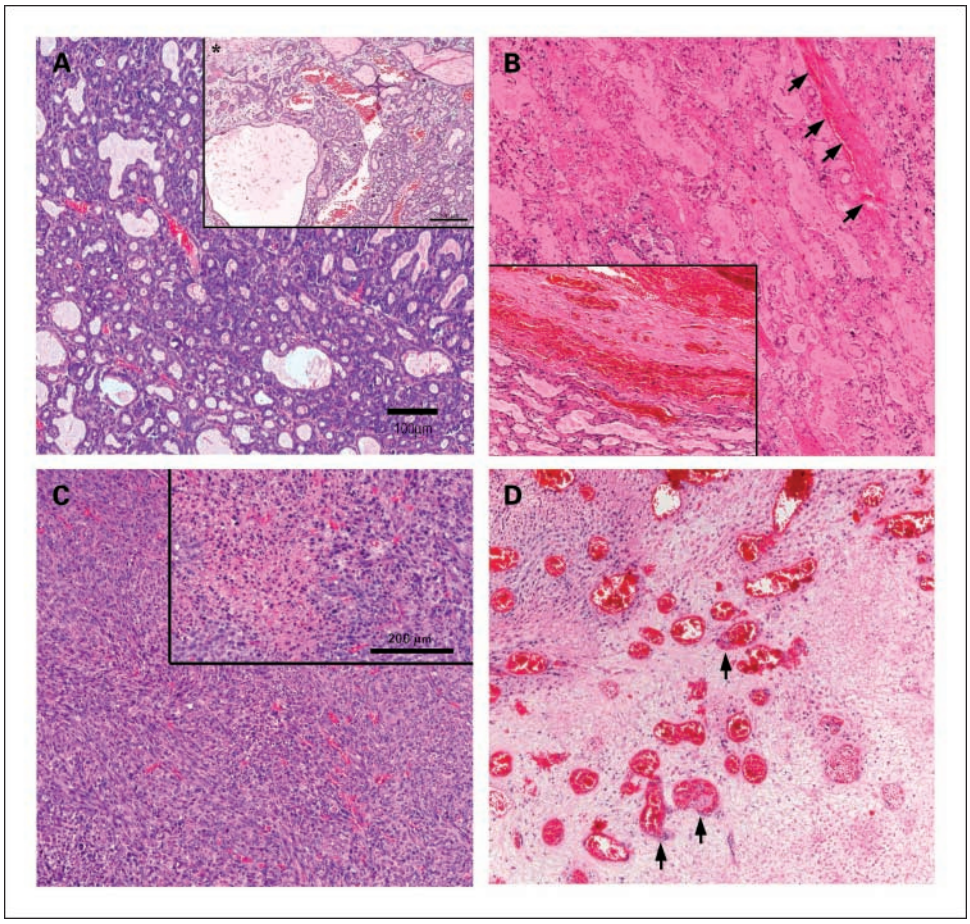

Fig. 3. Microphotographs (H&E staining) of well-differentiated tumors (*A* and *B*) and anaplastic tumors (*C* and *D*) before and 24 h post-PDT. *A,* mature vessels exist in well-differentiated tumor periphery, as well as tumor center. Inset, tumor center (bar, 200 μm; *, a necrotic lesion). Bar, 100 μm. *B,* PDT causes extensive hemorrhagic and coagulative necrosis in well-differentiated tumor with vascular stasis (*arrows*). Inset, evident hemorrhage and emboli in the tumor capsule. *C,* anaplastic tumor periphery and subperiphery area (*inset*) before PDT. There is evident cell necrosis in the tumor center due to poor perfusion. *D,* PDT destroys both vasculature (stasis and emboli) and tumor cells. Patches of viable cells are present.

Follow-up protocol and histologic study. After PDT, each rat was housed separately in a light-protected cage, with free access to food and water. Animals were monitored for any signs of toxicity or discomfort related to PDT, which included poor grooming, lethargy, and troubled breathing. Animals with signs of these distresses for 1 to 3 days were euthanized and subjected to necropsy. Tumor and major organs were retrieved for histologic examination. These euthanized rats were censored and tabulated as PDT/procedure-related death (see Table 1). Animals were otherwise followed for tumor growth delay/cure. Tumors were measured thrice per week with calipers in three mutually orthogonal diameters (D). Tumor volumes (V) were calculated using the formula $V = (\pi / 6) \times D_1 \times D_2 \times D_3$. When a tumor regrew to 4× treatment volume (end point), the rat was sacrificed and underwent necropsy looking for metastasis and changes in the tumor histology. Tumors that became impalpable for >100 days (for anaplastic tumors) or 200 days (for well-differentiated tumors) following treatment were considered cured. Tumor response (animal survival) to various therapy regimens was plotted as percentage of animals with tumor volume less than 4× treatment volume versus time after PDT.

Statistical analysis of survival data. The median survival days were calculated for each group using the Kaplan-Meier method (Prism). The multivariate Cox proportional hazards model (SAS ver. 9.1, SAS Institute, Inc.) was used to analyze the time for the tumor growth to 4× treatment volume with tumor sizes as covariates, because the pretreatment tumor size is an important factor affecting the tumor response to PDT. Premature deaths due to the treatment procedure were included in the model as censored cases. Hypotheses involved comparing continuous light delivery with fractionated light delivery. $P < 0.05$ was used for statistical significance.

Results

Histopathology findings and animal tolerance to interstitial PDT. In the initial PDT dose-finding experiments, animals bearing anaplastic tumors received escalated doses of light and QLT0074. One third (5 of 15) of the animals needed to be euthanized 3 to 5 days post-PDT with 2 mg/kg drug and 900 J fractionated light. These animals seemed to have succumbed from pulmonary edema possibly related to acute tumor necrosis. No gross pathologic changes in other organs were observed in these euthanized rats except for the lungs, in which capillary congestion with alveolar effusions was observed (data not shown). Therefore, intermediate PDT doses of 1.5 mg/kg drug and 900 J were chosen to compare continuous with fractionated light delivery. Subsequent animals tolerated the procedures well at the intermediate dose. During interstitial photodynamic therapy at light fluence rates used in this study, tumor temperatures (close to the fibers) increased from 34 ± 2°C (before PDT) to 36 ± 2°C (during PDT). Therefore, no hyperthermic effect on tumor response would be expected. All animals recovered from interstitial PDT, and none died within 24 h. However, the majority of animals manifested some degree of distress within 24 h post-PDT. Observed distress included decreased appetite and lethargy. Grossly, the skin over the tumor seemed swollen with ischemia. On acute histology, there was marked hemorrhagic reaction surrounding the tumor and inside the tumor (Fig. 2). Microscopically, the

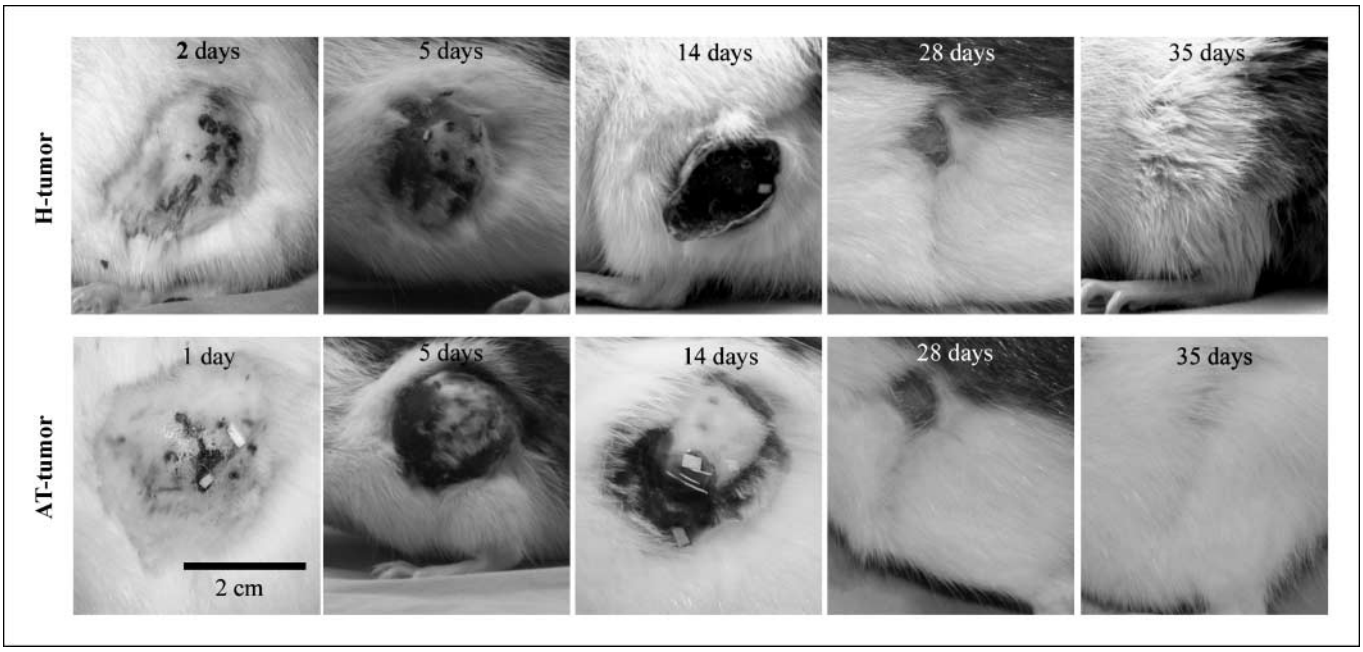

Fig. 4. Pictures showing time-course changes of an well-differentiated tumor (*H, top*) and an anaplastic tumor (*bottom*) treated by interstitial PDT with fractionated light delivery. Early changes (1-2 d) consisted of skin edema and tumor swelling with focal skin ischemia. The well-differentiated tumor started to shrink with extensive skin necrosis and escar formation 5 to 10 d post-PDT followed by tumor sloughing and skin healing. Necrosis of the anaplastic tumor was not as uniform as the well-differentiated tumor. Tumor ulcer formed after necrotic tumor tissue sloughed.

predominant damage of interstitial PDT was to the blood vessels and tumor *per se* (Fig. 3B and D). Vascular stasis and emboli were particularly evident in the larger capsular vessels. Coagulative tumor necrosis was observed in both tumor models; however, it was more comprehensive in well-differentiated than in anaplastic tumors (Fig. 3B and D). In the latter, sparing of viable tumor tissue was observed (Fig. 3D). As opposed to the initial swelling and subsequent tumor shrinkage observed for well-differentiated tumors post-PDT, the anaplastic tumors usually became ulcerated with sloughing of necrotic tumor tissue (Fig. 4). Despite this dramatic response, the majority of the anaplastic tumors regrew, leading us to conclude that those viable tumor cells either survived due to incomplete blood flow shutdown or to the ability of the anaplastic tumor to survive in hypoxic states (12).

Tumor perfusion changes. Figures 5 and 6 show representative DCE-MRI perfusion images of the well-differentiated and anaplastic tumors before and after PDT, with either fractionated or continuous light delivery, respectively. Images were acquired by dynamic three-dimensional volume scanning over 100 s immediately before (time, 0 s), during, and after contrast agent injection (the time for injection was 25-30 s). Before PDT, signal intensity enhancement (i.e., perfusion) in well-differentiated tumors was relatively homogeneous from tumor periphery to center (Fig. 5), indicating that well-differentiated tumor is well perfused, although there was intertumoral/intratumoral heterogeneity in tumors >4 cm^3. In contrast, perfusion in anaplastic tumors was highly inhomogeneous. The tumor periphery was well perfused, whereas the tumor center was poorly perfused (Fig. 6). Histologic findings of the well-differentiated and anaplastic tumors correlated well with these perfusion results. There was a noticeable necrotic center in anaplastic tumors of $\sim$2 cm^3, whereas only limited necrotic foci were observed in well-differentiated tumors of >5 cm^3 (Fig. 3A and C, insets). Furthermore, organized blood vessels were observed in both the periphery and center of well-differentiated tumors (Fig. 3A), but less dense and smaller vessels were observed in anaplastic tumors (Fig. 3C). Interestingly, after PDT with either fractionated or continuous light delivery, there was virtually no signal enhancement (perfusion) in both tumor sublines within 24 h (Figs. 5 and 6). This perfusion shutdown was further validated by MRI T1–spin echo images collected 5 min after dynamic imaging in anaplastic tumors (Fig. 6). This MRI perfusion data suggest that tumor vessel damage/stasis occurs early after PDT using either fractionated or continuous light delivery. These perfusion patterns are in agreement with previous tumor oxygenation studies using these tumor models (12, 29).

Time-course signal intensity curves were plotted from tumor rims of the well-differentiated and anaplastic tumors (Fig. 7A) and central slices of well-differentiated tumors (Fig. 7B) or anaplastic tumors (Fig. 7C) before and 1 h after PDT. Figure 7A shows that gadoteridol-induced signal enhancement in the tumor rim regions of interest reached peak levels from 70 to 100 s and was comparable in both tumor models before PDT. PDT with fractionated light delivery markedly reduced the signal enhancement to a level near baseline (time, 0 s). The percentage change (attenuation) in maximum gadoteridol intensity pretreatment and posttreatment was 80% in well-differentiated tumor periphery ($P < 0.0001$) and 78.5% in anaplastic tumor rim ($P < 0.0001$). PDT with continuous light delivery also reduced the perfusion of the tumor peripheries, with attenuation of 52% in the well-differentiated ($P = 0.0014$) and 74% in anaplastic tumors ($P < 0.0001$). Before PDT, the whole well-differentiated tumor perfusion was comparable with the tumor periphery (Fig. 7B). Figure 7B also shows the perfusion changes of the whole well-differentiated tumor posttreatment. PDT with fractionated light delivery and 1.5 mg/kg of QLT0074 greatly reduced the signal enhancement to near-baseline levels.

PDT with lower drug dose (1.0 mg/kg) and fractionated light or continuous light delivery also generated appreciable perfusion reduction, but to a lesser extent than 1.5 mg/kg. The average whole anaplastic tumor perfusion before PDT seemed much lower than that of its tumor rim, consistent with poor perfusion of the tumor center (Fig. 7C). PDT with either fractionated or continuous light delivery generated only a moderate attenuation of signal enhancement in anaplastic tumor, as there was virtually no perfusion in the tumor center pretreatment (Fig. 6). Unsurprisingly, treatment with light-only did not affect tumor perfusion. To examine when perfusion recovers, tumor perfusion from six rats (three bearing anaplastic and three bearing well-differentiated tumors) treated with fractionated light delivery was examined 72 h post-PDT. There was no evidence of perfusion recovery in these tumors (data not shown).

Animal survival. Figure 4 shows representative well-differentiated and anaplastic tumors cured by PDT with fractionated light delivery. Initially, post-PDT, both the well-differentiated and anaplastic tumors swelled with edema. The well-differentiated tumor started to shrink 5 to 10 days posttreatment with escar formation. The anaplastic tumor developed focal skin and tumor necrosis with ulceration. These macroscopic observations coincided with histologic changes observed post-PDT, in that damage to the well-differentiated tumor was more uniform relative to the anaplastic tumor (Fig. 3).

If the tumors were not cured, the time (in days) for tumor regrow to 4× treatment volume was recorded as the time of animal survival posttreatment. Survival curves of animals bearing anaplastic tumors are graphed in Fig. 8A and those bearing well-differentiated tumors in Fig. 8B. Generally, there was a dose-dependent tumor response to PDT in both tumor models. More importantly, animals treated with fractionated light delivery survived longer (taking a longer time to grow 4× treatment volume) than those treated with continuous light delivery when given the same PDT doses (1.5 mg/kg drug and 900 J per tumor). Using the Cox proportional hazards model to compute the *P* values and hazard ratios (HR) for tumors treated by fractionated light delivery relative to continuous light delivery (HR = 1), the *P* values and HRs for anaplastic and well-differentiated tumors were $P = 0.015$, HR = 0.29 (95% confidence interval, 0.10-0.79) and $P = 0.001$, HR = 0.28 (95% confidence interval, 0.10-0.74), respectively (see Table 1).

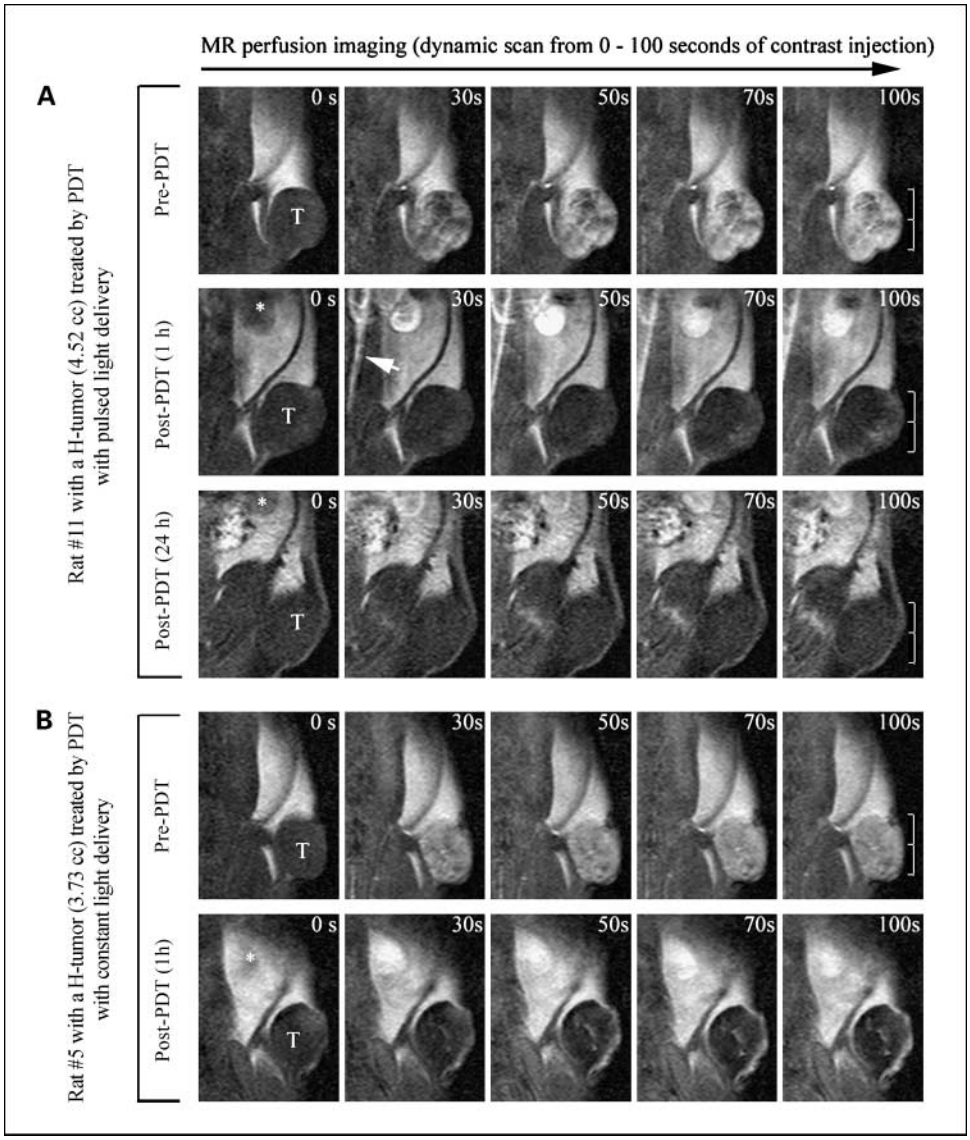

Fig. 5. DCE-MRI monitoring of well-differentiated tumor perfusion changes before and 1 to 24 h post-PDT. Gadolinium (contrast) was injected via the tail vein catheter after a baseline MRI scan of the tumor (time, 0 s). The tumor was dynamically scanned (repeated for 10 times) for 100 s. Slices shown are from 1 of the 10 sections of each tumor (see Materials and Methods for details of MRI scanning). *A*, a well-differentiated tumor (*T*) treated by PDT with fractionated light delivery. Before PDT, signal enhancement shows in 10 s and reaches a peak at 70 to 100 s from contrast injection. PDT significantly reduces the enhancement in the tumor. Contrast signal in the left kidney (*) and aorta artery (*arrow*) is clearly shown. The tumor outline is indistinctly 24 h post-PDT due to tumor edema. Bar, 2 cm. *B*, a well-differentiated tumor treated by PDT with continuous light delivery. Signal enhancement is homogenous before PDT. Post-PDT, there is a faint enhancement observed inside the tumor, as well as in the tumor rim.

Furthermore, tumor cures were observed only in groups receiving fractionated light delivery. Interestingly, for anaplastic tumors treated by shorter light-on cycles (1 s per fiber per cycle), there was no statistical significance in survival between groups of fractionated and continuous light delivery ($P = 0.229$, HR = 0.55). However, for well-differentiated tumors treated by shorter light-on cycles (5 s per fiber), there was a statistical difference between groups of fractionated and continuous light delivery ($P = 0.001$, HR = 0.31). Therefore, fractionated light delivery for PDT may work even better in well-perfused well-differentiated tumors. Tumor size was also a critical factor affecting tumor response. PDT at a fix dose was clearly less effective for the larger tumors. The HRs of tumors ≥ 4 cm^3 relative to tumors <4 cm^3 were 1.88 and 3.40 for well-differentiated and anaplastic tumors, respectively. The average tumor sizes were comparable among different groups within each tumor type (see Table 1), except for the initial high-dose anaplastic tumor group.

Discussion

This study shows that fractionated light delivery is more effective than continuous light delivery in interstitial PDT of solid tumors (rat prostate carcinomas). Here, we used two extremes of tumor differentiation and perfusion to examine the tumor response. DCE-MRI was used in this study to gain more anatomic information over previous studies and consistent with other studies is a suitable method for providing noninvasive assessment of tumor perfusion changes pre-PDT and post-PDT (21, 30). The rationale of fractionated light delivery is that it will allow tissue reoxygenation to occur during the light-off period, extending direct phototoxicity to tumor cells at the early phase of PDT (10, 15, 17). The rate of O_2 consumption in the photodynamic process is believed to be fast and in the order of seconds (31, 32). To date, however, the optimal fractionation rates have not been clearly defined (33). At the late phase of PDT, when the tumor vessels are damaged and blood flow stops, the phototoxicity benefit from fractionated light delivery is likely minimal. The advantage of computer-switched fractionated light delivery with multiple interstitial fibers is that fractionated light can be constantly delivered to the tumor or target organ in various sequences of on/off durations. This may be important as the blood flow and O_2 delivery changes overtime, with a reported initial increase and then decrease (34). Potentially, this change in blood flow and oxygenation can be monitored by sequential illumination and detection in the multifiber array and the duration of on/off sequences adjusted. Furthermore, real-time photosensitizer fluorescence

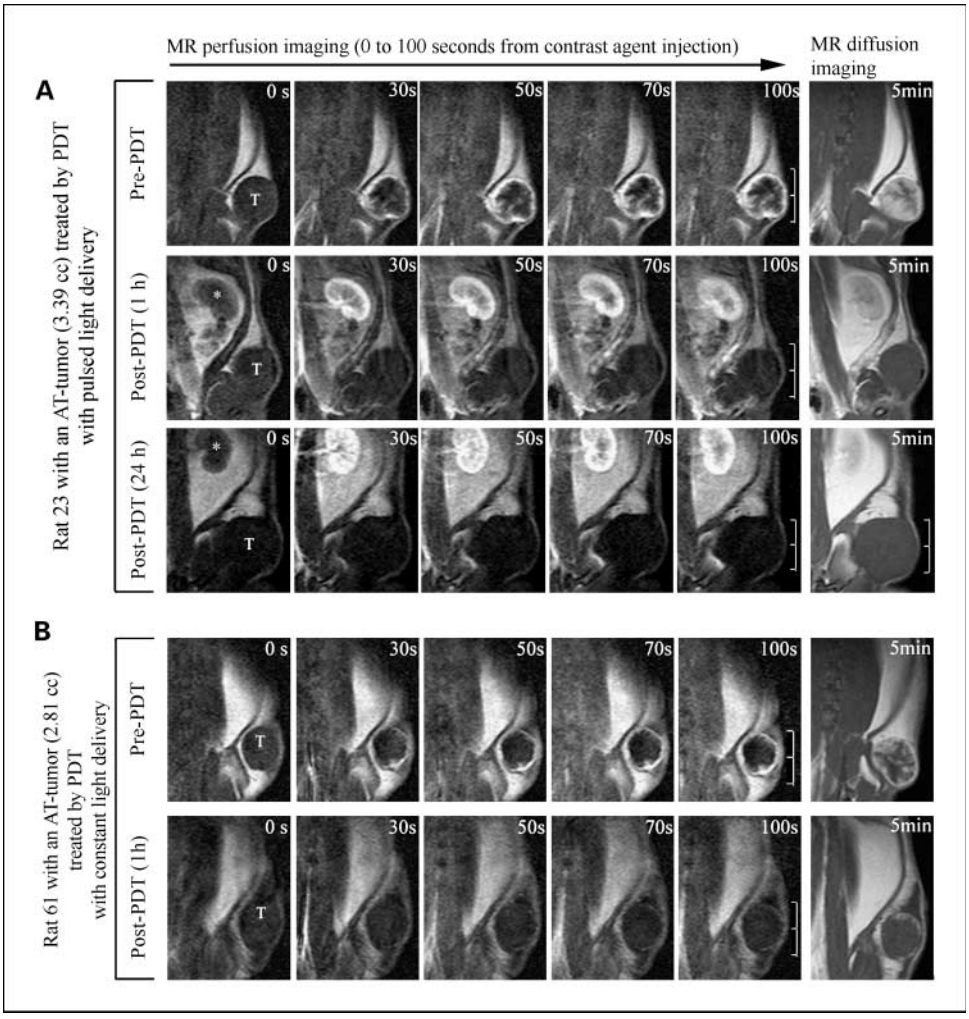

Fig. 6. DCE-MRI monitoring of anaplastic tumor perfusion changes before and 1 to 24 h post-PDT. *A*, an anaplastic tumor on the left flank treated by PDT with fractionated light delivery. Before PDT, perfusion in this tumor is highly inhomogeneous; the tumor rim is well perfused, whereas the tumor center is poorly perfused (no enhancement). PDT markedly reduces perfusion of the tumor periphery. Tumor volume increases 24 h post-PDT (edema). *B*, an anaplastic tumor treated by PDT with continuous light delivery. The changes are similar to that in the top (bar, 2 cm). At 5 min after the dynamic scans, MRI T1 – spin echo scanning was done to detect contrast diffusion from the perfused anaplastic tumor periphery. Contrast diffusion was observed in tumors before PDT but not observed post-PDT, suggesting PDT damage to the tumor vasculature.

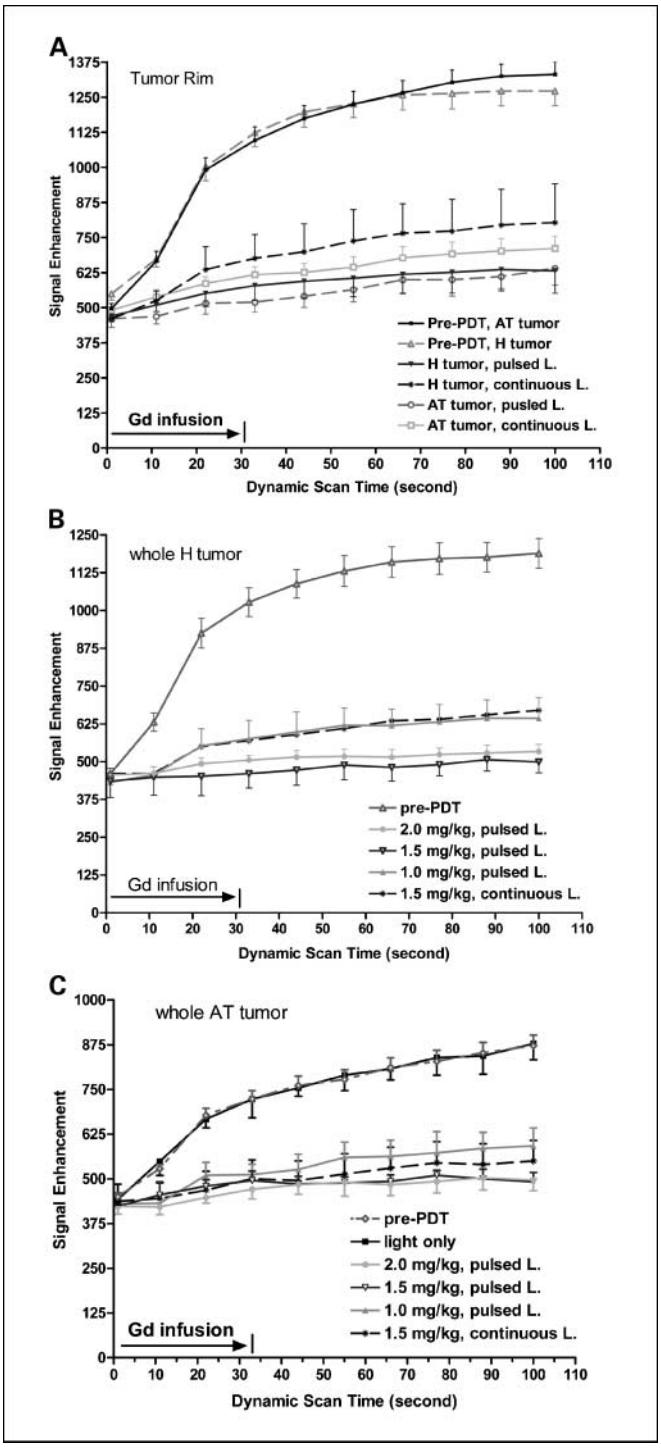

Fig. 7. MRI signal enhancement time-course curves before and 1 h after interstitial PDT. Signal intensity at time 0 is the baseline tumor intensity, before gadoteridol (*Gd*) injection. Points, average results from each group; bars, SEs. *A,* time-course curves of signal enhancement in tumor rims of anaplastic and well-differentiated tumors. Before PDT, signal enhancement reached the maximum at 70 to 90 s from contrast injection. PDT with fractionated light delivery reduced the enhancement to the baseline level. PDT with continuous light delivery also significantly reduced the enhancement in both tumor sublines. *B,* time course curves of signal enhancement in well-differentiated tumors (whole central slices). The signal enhancement in the tumor center was comparable with that of the tumor periphery before PDT. PDT significantly reduced the enhancement of the whole tumor. *C,* time-course curves of signal enhancement in anaplastic tumors (whole central slices). Because there is virtually no enhancement in the tumor center, the changed values shown here are the averaged intensity from the tumor rim. Tumors treated with light-only did not generate any perfusion changes.

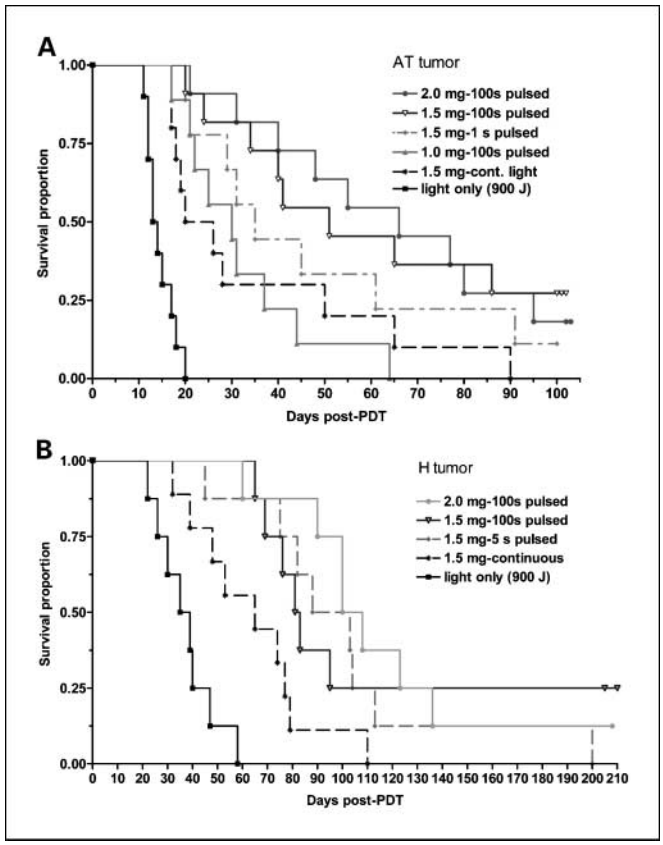

Fig. 8. Survival of rats bearing anaplastic and well-differentiated prostate tumors treated by interstitial PDT with fractionated or continuous light delivery. See Table 1 for details of statistical analysis. *A,* Kaplan Meier survival curves of rats bearing anaplastic tumors treated by interstitial PDT with fractionated or continuous light or light-only (control). Survival is significantly different for rats treated with fractionated light compared with continuous light ($P = 0.015$, HR = 0.29). *B,* Kaplan Meier survival curves of rats bearing well-differentiated tumors treated by interstitial PDT with fractionated or continuous light or light-only (control). Survival is statistically different for rats treated with fractionated light delivery related to continuous light delivery ($P = 0.001$, HR = 0.28).

detection in tumor is possible, thereby customizing light dosimetry, as much as possible, to shape PDT effect (35).

The O_2 recovery phase (light off) is likely to be tumor type dependent owing to variations in vessel structure (density), flow rate, and oxygenation. For anaplastic tumors, the 1-s on (6-s off) cycles showed less effective response than the 100-s on (600-s off) cycles. On the other hand, for well-differentiated tumors, the 5-s on (30-s off) cycles were as effective as the 100-s on cycles. This finding may be consistent with the better oxygenation status of the well-differentiated tumor. Although not thoroughly explored, a light-off period of 100 s seems to be optimal for O_2 recovery in both the well-differentiated and anaplastic tumors. It should be kept in mind, with this iterative switch system, that the longer the light-off period, the longer the light-on time. Previous tumor oxygen tension measurement studies showed that continuous irradiation of 2 min could reduce the tumor oxygen to near zero (10, 17, 32). Given these time intervals, we tried to use two laser sources simultaneously to speed up the treatment. Interestingly, similar tumor response and tumor temperature changes were observed between one and two sources (data not shown).

In this particular study, we elected to use DCE-MRI to monitor the extent of PDT-induced vascular effect. DCE-MRI is

based on the concept that if the vessel becomes collapsed either due to vasospasm, vascular stasis, or posttreatment necrosis, the subsequently injected contrast medium cannot be delivered into that tissue to show enhancement. The three-dimensional gradient DCE-MRI technique was applied in this study to monitor tumor perfusion changes before and after interstitial PDT. Baseline perfusion studies (pre-PDT) showed the well-differentiated tumor to be well perfused, with a relatively homogeneous distribution of gadoteridol from the tumor periphery to the center. In contrast, the anaplastic tumors were poorly perfused with only the tumor periphery being well perfused (pre-PDT). Additionally, larger tumors had proportionately greater hypoxic/necrotic volumes with increased heterogeneity in tumor perfusion. However, differences in vessel patterns and tumor perfusion may exist between heterotopic and orthotopic prostate tumor models. PDT markedly reduced the perfusion of the anaplastic tumor rim and the whole well-differentiated tumor. Therefore, vascular shutdown is a major mechanism contributing to QLT0074-PDT phototoxicity in these heterotopic models. Histologic examination not only confirmed tumor vascular stasis but also showed substantial tumor cell damage. PDT with fractionated light tended to produce a greater reduction in perfusion compared with continuous light delivery, suggesting the former procedure eventually causes more vascular damage. This is in agreement with the observed tumor response (animal survival).

Although photodynamic therapy of the prostate is still experimental, our ultimate goal is to treat the whole prostate (benign or cancerous diseases) with targeted light and drug delivery. Our proposed intraarterial drug delivery will require real-time monitoring drug delivery and accurate light dosimetry (13). This switched/fractionated delivery system should allow us to accomplish this goal with proposed iterative feedback monitoring the amount of drug, light, fluorescence, and deoxyhemoglobin. In future clinical applications of PDT, the light and drug doses should be carefully prescribed to achieve a targeted or optimal effect.

In summary, this investigation shows, in two differently perfused animal tumor models of the prostate cancer, that PDT with computer-switched/fractionated light delivery is more effective compared with conventional/continuous light delivery. It also shows that DCE-MRI provides noninvasive assessment of tumor perfusion changes before and after treatment, which correlate with phototoxicity to the tumor both histologically and by survival. Fractionated light delivery, is therefore likely to improve efficacy in clinical PDT of solid tumors, while allowing for iterative monitoring using the multifiber switched delivery method. The light-on period for each fiber will need to exceed 5 s in cycles and will likely need to be worked out for each individual tumor, ideally in a real-time process to maximize the PDT effect.

Acknowledgments

We thank I. Piva, D. Jeske, and K. Kvamme for MRI imaging of the animals, and John Hanson at the Public Health Institute, Alberta Cancer Board, for performing the statistical analysis. The photosensitizer QLT0074 was supplied free of charge from QLT, Inc.

References

1. Jemal A, Siegel R, Ward E, et al. Cancer statistics, 2007. CA Cancer J Clin 2007;57:43–66.
2. Carter HB. Prostate cancers in men with low PSA levels - must we find them? N Engl J Med 2004;350:2292–4.
3. D'Amico AV, Chen MH, Roehl KA, Catalona WJ. Preoperative PSA velocity and the risk of death from prostate cancer after radical prostatectomy. N Engl J Med 2004;351:125–35.
4. Stamey TA, Caldwell M, McNeal JE, Nolley R, Hemenez M, Downs J. The prostate antigen era in the United States is over for prostate cancer: what happened in the last 20 years? J Urol 2004;172:1297–301.
5. Doughery TJ, Gomer CJ, Henderson BW, et al. Photodynamic therapy. J Natl Cancer Inst 1998;90:889–905.
6. Nathan TR, Whitelaw BE, Chang SC, et al. Photodynamic therapy for prostate cancer recurrence after radiotherapy: a phase I study. J Urol 2002;168:1427–32.
7. Gibson SL, Van Der Meid KR, Murant RS, Raubertas RF, Hiff R. Effects of various photoradiation regimens on the antitumor efficacy of photodynamic therapy for R3230AC mammary carcinoma. Cancer Res 1990;50:7236–41.
8. Henderson BW, Busch TM, Vaughan LA, et al. Photofrin photodynamic therapy can significantly deplete or preserve oxygenation in human basal cell carcinomas during treatment, depending on fluence rate. Cancer Res 2000;60:525–9.
9. Sitnik TM, Hampton JA, Henderson BW. Reduction of tumor oxygenation during and after photodynamic therapy *in vivo*: effects of fluence rate. Br J Cancer 1998;77:1386–94.
10. Tromberg BJ, Orenstein A, Kimel S, et al. *In vivo* tumor oxygen tension measurements for the evaluation of the efficiency of photodynamic therapy. Photochem Photobiol 1990;52:375–85.
11. Fingar VH, Wieman TJ, Wiehle SA, Cerrito PB. The role of microvascular damage in photodynamic therapy: the effect of treatment on vessel constriction, permeability, and leukocyte adhesion. Cancer Res 1992;52:4914–21.
12. Moore RB, Chapman JD, Mercer JR, et al. Measurement of PDT-induced hypoxia in Dunning prostate tumors by iodine-123-iodoazomycin arabinoside. J Nucl Med 1993;34:405–13.
13. Xiao Z, Dickey D, Owen RJ, Tulip J, Moore RB. Interstitial photodynamic therapy of the canine prostate using intra-arterial administration of photosensitizer and computerized pulsed light delivery. J Urol 2007;178:308–13.
14. Chen Q, Huang Z, Chen H, Shapiro H, Beckers J, Hetzel FW. Improvement of tumor response by manipulation of tumor oxygenation during photodynamic therapy. Photochem Photobiol 2002;76:197–203.
15. Iinuma S, Schomacker KT, Wagnieres G, et al. *In vivo* fluence rate and fractionation effects on tumor response and photobleaching: photodynamic therapy of two photosensitizers in an orthotopic rat tumor model. Cancer Res 1999;59:6164–70.
16. Vaupel P, Schlenger K, Knoop C, Höckel M. Oxygenation of human tumors: evaluation of tissue oxygen distribution in breast cancers by computerized O_2 tension measurements. Cancer Res 1991;51:3316–22.
17. Pogue BW, Braun RD, Lanzen JL, Erickson C, Dewhirst MW. Analysis of the heterogeneity of pO_2 dynamic during photodynamic therapy with verteporfin. Photochem Photobiol 2001;74:700–6.
18. Chen Q, Chen H, Hetzel FW. Tumor oxygenation changes post-photodynamic therapy. Photochem Photobiol 1996;63:128–31.
19. Kennedy SD, Szczepaniak LS, Gibson SL, Hilf R, Foster TH, Bryant RG. Quantitative MRI of Gd-DTPA uptake in tumor: response to photodynamic therapy. Magn Reson Med 1994;31:292–301.
20. Su MY, Samoszuk MK, Wang J, Nalcioglu O. Assessment of protamine-induced thrombosis of tumor vessels for cancer therapy using dynamic contrast-enhanced MRI. NMR Biomed 2002;15:106–13.
21. Gross S, Gilead A, Scherz A, Neeman M, Salomon Y. Monitoring photodynamic therapy of solid tumors online by BOLD-contrast MRI. Nat Med 2003;9:1327–31.
22. Isaacs JT. Development and characteristics of the available animal model systems for the study of prostate cancer. In: Coffey DS, Bruchovsky N, Gardener WA, Resnick MI, Cur JP, editors. Current concepts and approaches to the study of prostate cancer. New York: Alan R. Liss; 1987. p. 513–76.
23. Thorndyke C, Meeker BE, Thomas G, Lakey WH, McPhee MS, Chapman JD. The radiation sensitivities of R3327-H and R3327-AT rat prostate adenocarcinomas. J Urol 1985;134:191–8.
24. Chapman JD, McPhee MS, Walz N, et al. Nuclear magnetic resonance spectroscopy and sensitizer-adduct measurements of photodynamic therapy-induced ischemia in solid tumors. J Natl Cancer Inst 1991;83:1650–9.
25. Xiao Z, Tamimi Y, Brown K, Tulip J, Moore R. Interstitial photodynamic therapy in subcutaneously implanted urologic tumors in rats after intravenous administration of 5-aminolevulinic acid. Urol Oncol 2002;7:125–32.
26. Granville DJ, Hunt DWC. Porphyrin-mediated

photosensitization - taking the apoptosis fast lane. Curr Opin Drug Discov Devel 2000;3:232–43.

27. Richter AM, Waterfield E, Jain AK, Canaan AJ, Allison BA, Levy JG. Liposomal delivery of a photosensitizer, benzoporphyrin derivative monoacid ring A (BPD), to tumor tissue in a mouse tumor model. Photochem Photobiol 1993;57:1000–6.

28. Richter AM, Waterfield E, Jain AK, et al. Photosensitizing potency of structural analogues of benzoporphyrin derivatives (BPD) in a mouse tumor model. Br J Cancer 1991;63:87–93.

29. Zhao D, Ran S, Constantinescu A, Hahn EW, Mason RP. Tumor oxygen dynamics: correlation of *in vivo* MRI with histological findings. Neoplasia 2003;5:308–18.

30. Fei B, Wang H, Muzic RF, Jr., et al. Deformable and rigid registration of MRI and microPET images for photodynamic therapy of cancer in mice. Med Phys 2006;33:753–60.

31. Foster TH, Murant RS, Bryant RG, Knox RS, Gibson SL, Hilf R. Oxygen consumption and diffusion effects in photodynamic therapy. Radiat Res 1991;126:296–303.

32. Zilberstein J, Bromberg A, Frantz A, et al. Light-dependent oxygen consumption in bacteriochlorophyll-serine-treated melanoma tumors: on-line determination using a tissue-inserted oxygen microsensor. Photochem Photobiol 1997;65:1012–9.

33. Henderson BW, Busch TM, Snyder JW. Fluence rate as a modulator of PDT mechanisms. Lasers Surg Med 2006;38:489–93.

34. Busch TM. Local physiological changes during photodynamic therapy. Lasers Surg Med 2006;38:494–9.

35. Dickey DJ, Partridge K, Moore RB, Tulip J. Light dosimetry for multiple cylindrical diffusing source for the use in photodynamic therapy. Phys Med Biol 2004;49:3197–208.